INVESTIGATIONS OF ELECTRON EMISSION CHARACTERISTICS OF LOW WORK FUNCTION SURFACES

Report No. 1

by

L. W. Swanson
A. E. Bell
I. C. Crouser
B. E. Evans

Prepared for

Headquarters
National Aeronautics and Space Administration
Washington, D. C.

Quarterly Report No. 1
28 September to 27 December 1966

February 1967

CONTRACT NASw-1516

FIELD EMISSION CORPORATION
Melrose Avenue at Linke Street
McMinnville, Oregon 97128

TABLE OF CONTENTS

LIST OF ILLUSTRATIONS

PURPOSE

The primary aims of this investigation are to obtain an improved fundamental understanding of (1) the phenomena governing the production of low work function surfaces, and (2) the factors affecting the quality and stability of electron emission characteristics. It is expected that the information generated from this investigation will be relevant to various kinds of electron emission (i. e., photo, thermionic and field emission), although the primary emphasis will be placed upon field emission. Accordingly, field emission techniques will be employed, at least initially, to obtain the objectives of this work.

The formation of low work function surfaces will be accomplished by: (1) adsorption of appropriate electro-positive adsorbates, (2) coadsorption of appropriate electropositive and electronegative adsorbates, and (3) fabrication of emitters of low work function surfaces from various metalloid compounds. Various properties of these surfaces to be investigated in order to obtain a more fundamental understanding of them are the temperature dependency of the emission and work function, the various types of energy exchanges accompanying emission, the energy distribution of the field emitted electron, and various aspects of the surface kinetics of adsorbed layers such as binding energy, surface mobility and effect of external fields.

ABSTRACT

A field emission study of cesium and fluorine coadsorbed on tungsten is reported. Work function minima as low as 1.0 eV are reported along with the effect of coadsorbed fluorine on the migration and desorption rates of cesium. Although cesium can be thermally desorbed throughout most of the coverage range from a fluorinated tungsten surface without disturbing the underlying fluorine layer, there is evidence that at low cesium coverages thermal desorption of cesium enhances the removal of the otherwise stable fluorine layer.

Also reported is a study of the mechanisms leading to decay of field emission current from a low work function zirconium/oxygen coated tungsten emitter. The results obtained thus far indicate electron induced desorption of neutral and ionic particles from anode surfaces, which impinge on the emitter surface, as the main cause of the time decay of field emission current.

COADSORPTION OF CESIUM AND FLUORINE ON TUNGSTEN

INTRODUCTION

Studies of coadsorption of alkali metals and electronegative gases on refractory metal substrates reveal that the minimum work functions obtained are lower than those using alkali adsorbates alone. Work function lowering of approximately 3.0 eV is obtained with cesium alone adsorbed on tungsten, while a net decrease of approximately 3.5 eV is obtainable with cesium adsorbed on a preadsorbed layer of oxygen[1,2]. In addition, the Cs becomes more tightly bound to the substrate when O is present. A consideration of the pertinent physical properties shown in Table I suggests that the extreme adsorbates, Cesium and Fluorine, might yield even lower work functions.

TABLE I

Physical Properties of Oxygen and Fluorine

	Ionization Potential (Volts)	Atomic Radius (A^o)	Electonegativity Pauling Scale (eV)	Electron Affinity (Volts)
O	13.55	0.60	3.5	1.46
F	17.34	0.50	4.0	3.46

An earlier field emission study of the Cs/F/W system by Wolf[3] yielded work function minima as low as 1.1 eV using a heatable bucket from which CsF could be sublimed onto a tungsten field emitter. He also found that Cs could be desorbed and a coverage of F retained on the tip by depositing CsF on an emitter held at 1200°K.

Previously, we reported[4] similar results for the same system and preliminary results for a similar study which included an additional source for the deposition of Cs. The ability of F to reduce the work function minimum was clearly demonstrated. Work functions of 0.97 eV, stable up to 500°K

were obtained. Migration studies indicated dissociative adsorption of CsF so that migration of Cs occurred in the usual range of 150-250°K, while F did not become mobile until $T > 380^{\circ}K$. It was also reported that adsorption and desorption of Cs on a F/W layer was completely reversible, leaving the F/W layer unchanged. More complete studies now show that the latter is true only when a positive electric field, i. e., the screen negative, is applied while heating.

Finally, the low work function (1. 2 - 2. 0 eV) field emission patterns obtained by deposition of CsF were characterized by bright 112 planes which gradually diminished in brightness at temperatures as low as 78°K when a field emission potential was applied to the tip. The behavior was explained in terms of field desorption of F^-.

The work in this quarter has been primarily on separate adsorption of cesium on an underlying F/W layer. Data has been obtained on the formation of a F/W layer and its stability in the presence of Cs, migration of cesium on F/W, work function versus Cs coverage at various underlying F coverages using calibrated Cs doses and desorption temperatures versus Cs coverage for clean and F covered W.

EXPERIMENTAL

The construction of the field emission microscope for the coadsorption study shown in Figure 1 was standard except for provisions made to measure and control the emitter temperature[6]. Pattern viewing was accomplished by pulse techniques to eliminate any field effects due to viewing voltage. The tip temperature is derived from an accurate measurement of the resistance of a small section of the emitter's supporting filament C. This makes use of the fact that the resistivity of W is a well-known, monotonic, and nearly linear function of temperature over the range of interest. The resistance of a segment of the loop was determined by passing an accurately known dc current through it and measuring the potential difference across it by means of two small leads attached to the filament. The resistance was

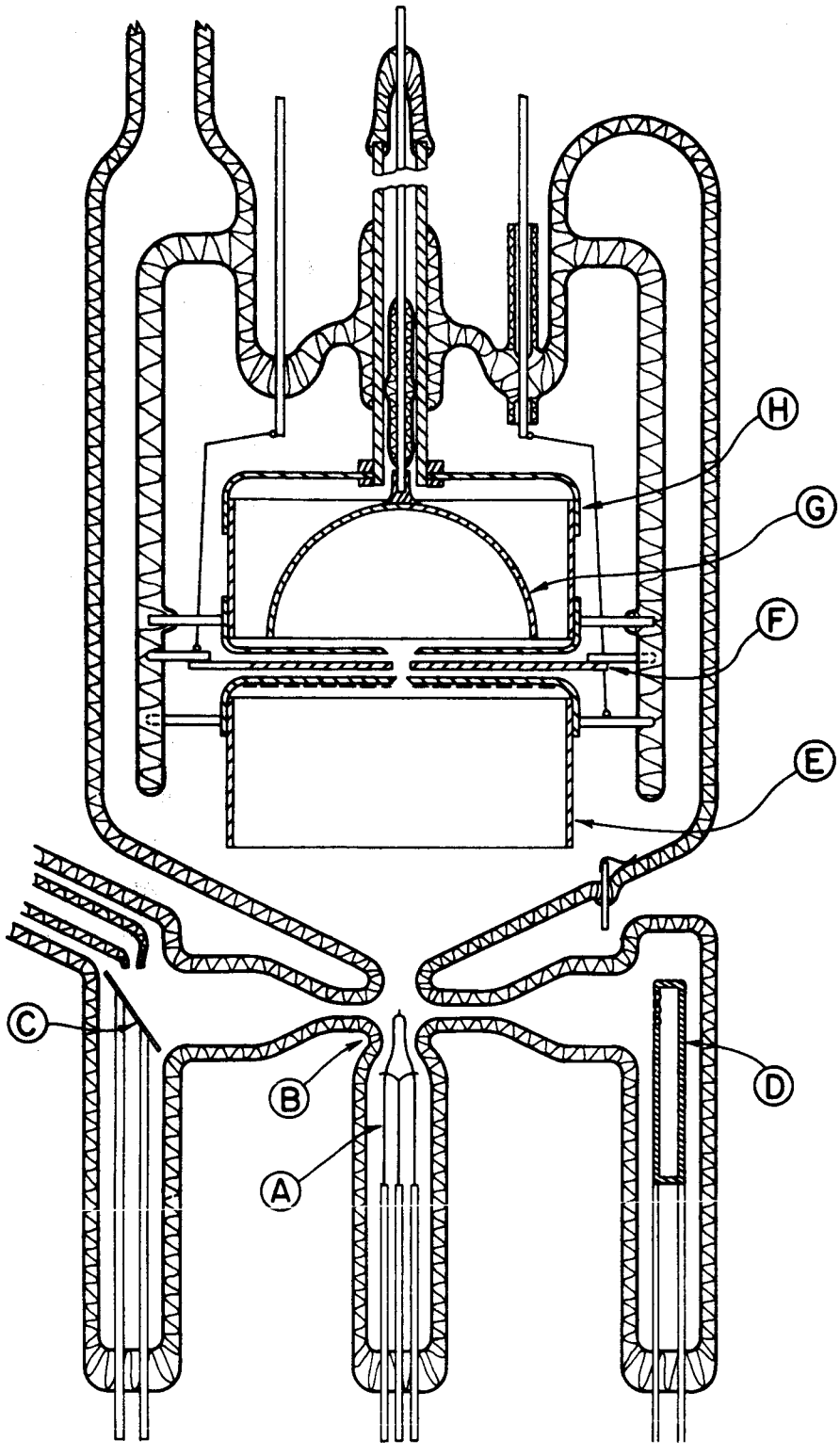

Figure 1. Diagram of coadsorption magnetic deflection probe tube. Tube contains following components:

(A) emitter assembly	(E) anode
(B) space for electromagnet	(F) lens electrode
(C) cesium source platform	(G) spherical collector
(D) oxygen source	(H) Faraday cage

calibrated by measuring it at several well-determined temperatures.

The tube shown in Figure 1 contains a Cs source consisting of a platinum disc onto which Cs was condensed and subsequently sublimed onto the tip by controlled resistive heating of the disc. The CsF source consisted of optical grade crystals which were thoroughly outgassed during tube evacuation by placing them in a resistively heated platinum bucket. After seal off the tube was placed in a liquid N_2 cryostat; CsF could be deposited onto the emitter in pure form by heating the platinum bucket to $\sim 900^{\circ}K$.

The application of the field emission microscope to an investigation of the work function change of various substrates on adsorption is made possible by the well-known and experimentally confirmed Fowler-Nordheim law of field emission. This law may be expressed in terms of the directly measurable field emission current I and applied field F_a as

$$I = \frac{BF_a^2}{\phi t^2(\phi, F_a)} \exp\left[-\frac{b\phi^{3/2} v(\phi, F_a)}{F_a}\right] \qquad (1)$$

where $t(\phi, F)$ and $v(\phi, F)$ are tabulated nondimensional functions which take into account the image correction, B is proportional to emitting area, and $b = 6.8 \times 10^7$ where F_a is in V/cm, and ϕ in eV. Although Equation (1) is the zero-degree temperature approximation, it holds reasonably well at higher temperatures provided ϕ is sufficiently large. By defining the field factor $\beta = F_a/V$ where V is the applied voltage, Equation (1) may also be written as:

$$\ln I/V^2 = \ln A + m/V, \qquad (2)$$

where A is the intercept and m is the slope of a "Fowler-Nordheim" plot of the I(V) data plotted in the form $\ln I/V^2$ vs I/V. The slope m may be written as follows:

$$m = -\frac{b\phi^{3/2} s(\phi, F_a)}{\beta} \qquad (3)$$

where $s(\phi, F_a)$ is another tabulated function. In the range of F_a and ϕ, encountered in this investigation Equations (1) and (3) may be simplified by the following close approximation:

$$v(\phi, F_a) = 0.943 - 0.146 \times 10^{-6} F/\phi^2 \qquad (4)$$

from which it can be easily shown that $s(\phi, F) = 0.943$. Using the known work function ϕ_s of the clean surface as a reference, and assuming β to be unchanged by adsorption, the work function ϕ at the surface when coated with an adsorbate can then be determined from Equation (3) written as follows:

$$\phi = \phi_s \left[\frac{m\, s(\phi, F_a)}{m_s\, s(\phi_s, F_a)} \right]^{2/3}, \qquad (5)$$

where m_s and m are the slopes of the corresponding Fowler-Nordheim plots.

Formation of a F/W Layer. - A F/W surface was formed by electrically heating the platinum bucket from which CsF was sublimed onto the emitter. Subsequent heating of the emitter up to 1100°K migrated the adsorbate across the emitter and removed only the Cs by thermal desorption provided the tip was maintained at a positive potential relative to the screen during heating. The F layer thus formed could be retained on the emitter surface at temperatures up to 1400°K independent of the potential applied to the emitter provided it was not further exposed to Cs. Figure (2) shows a plot of work function and the Fowler-Nordheim preexponential log A versus the number of CsF doses deposited on the emitter and subsequently equilibrated at 1100°K in order to remove Cs. Doses 1 through 8 were done with no electric field applied to the emitter, while doses 8 through 14 were equilibrated with the screen held at -225 V during the heating period. The corresponding field strength was approximately 2.4×10^6 V/cm. Following dose 14, the tip was heated to 1100°K for five minutes and the work function remained constant.

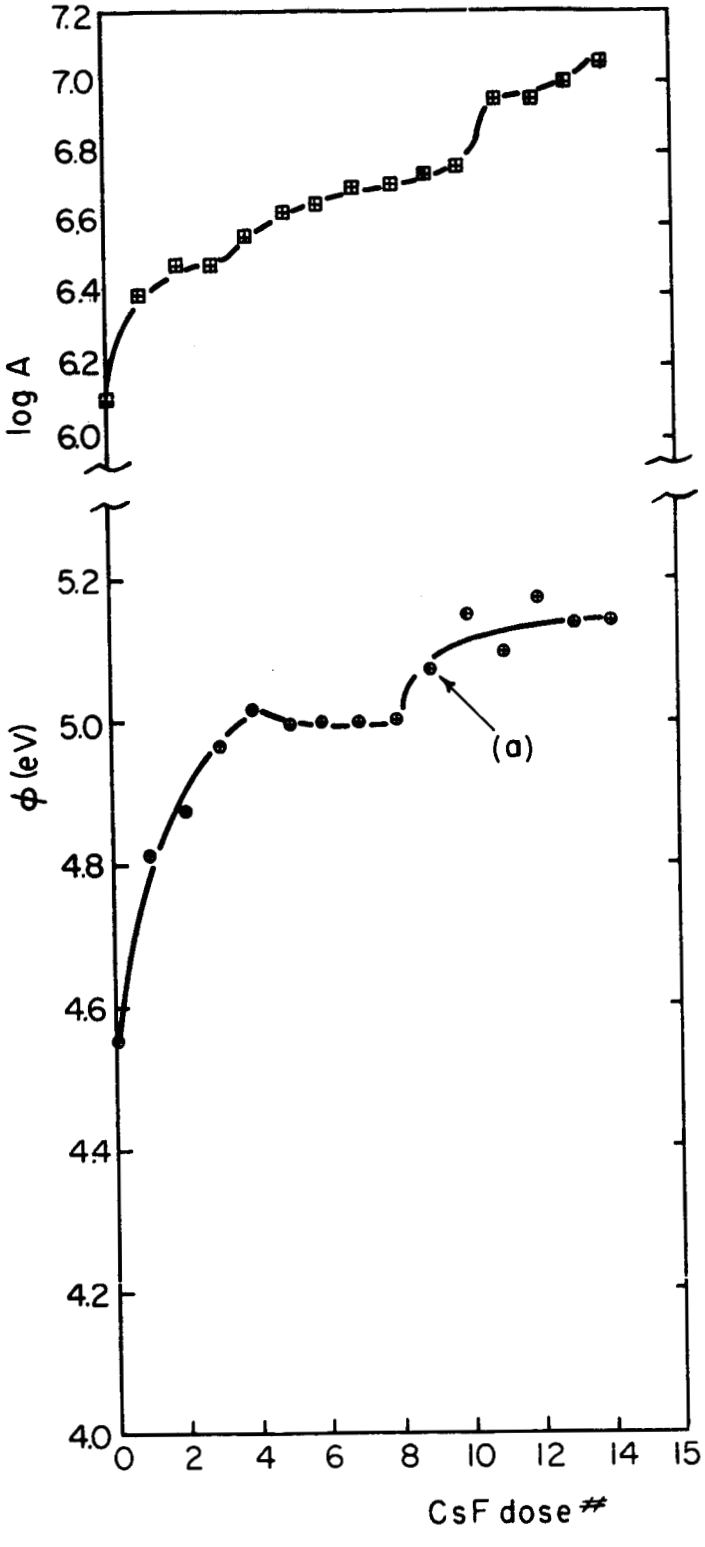

Figure 2. Curves show variation of ϕ and log A with CsF dose number. At (a) -200 V was applied to the screen during the 1100°K equilibration.

Temperatures greater than 1400°K were required to ultimately remove the F layer thus formed. Further exposure to cesium followed by heating at 1100°K with no field applied to the emitter tip reduced the work function from its maximum value of 5.14 to 4.90 eV. It was, therefore, concluded that F alone cannot be removed from W below 1400°K; but that it can be removed below 1100°K in the presence of Cs, presumably by evaporation as CsF.

Work Function Change. - During the deposition of Cs on clean W the temperature T_e required to equilibrate (i.e., to migrate the cesium across the emitter surface) each dose was noted. Upon equilibrating each dose, the work function was determined from the slope of a Fowler-Nordheim plot according to Equations (2) and (3). From previous knowledge of the ϕ versus Cs coverage σ on clean W, the dose size could be established. A repetition of this procedure at various underlying F coverages yielded the family of curves shown in Figure 3, where the lower set is the ϕ versus σ curves, the middle group shows the variation of log A with σ and the upper group of curves show the variation of T_e with σ.

From the Figure 3 results it is clear that the presence of an underlying F layer significantly reduces the minimum work function obtainable by cesium adsorption. In contrast to the Cs/O/W system, the value of σ at ϕ_{min} remains essentially unchanged. We further note that whereas a O/W layer corresponding to ϕ = 5.65 eV was required to produce a minimum work function of 1.1 eV, in the case of the F/W layer, an initial work function of 5.14 eV leads to a work function of 1.0 eV. In view of the larger value of electron affinity for F than for O, it is very likely that dipole moments for F are larger, so that the F coverage is smaller than the O coverage at identical values of $\Delta\phi$. Thus we conclude that a F layer affects a larger net work function lowering with Cs than an O layer at corresponding coverages.

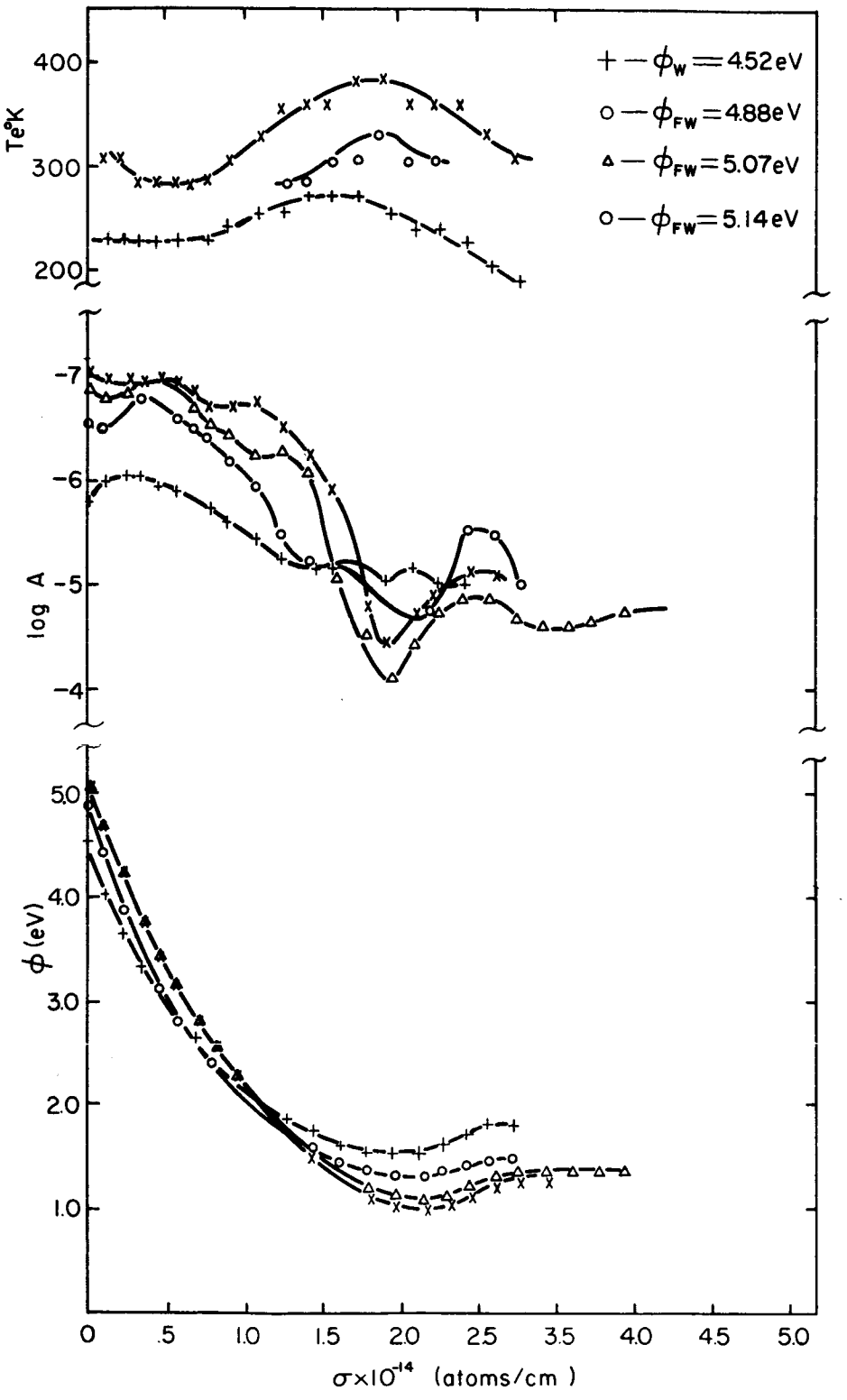

Figure 3. Lower set of curves show variation of work function with Cs coverage for clean and fluorine coated tungsten. Middle set of curves shows the variation of log A and upper set shows the variation of the equilibration temperature T_e with Cs coverage.

Migration of Cs on F/W. - After each deposit of Cs on the emitter, the tip was heated for 60 second intervals at successively increasing temperatures. Between each interval the tip was cooled to 78°K and the symmetry of the pattern was noted along with the voltage required to produce a given field emission current. The temperature above which the pattern was symmetric was noted as the equilibration temperature T_e. At higher temperatures the work function continued to change until the emitter shank was also equilibrated as indicated by a leveling off of the work function change with time.

A plot of the emitter equilibration temperature versus cesium coverage is shown in Figure 3 for clean W and for two underlying F coverages. From these curves it can be observed that the underlying F layer raises the temperature required for migration of Cs in a fashion similar to that reported for the Cs/O/W system[1,2].

Thermal Desorption. - At the end of each adsorption sequence the emitter was heated for 60 second intervals at successively increasing temperatures up to 2000°K. The work functions were measured between intervals and a plot of the work function versus heating temperature was obtained as shown in Figure 4. A summary of the significant features of the adsorption curves and the corresponding desorption curves is given in Table II.

TABLE II

Summary of Figure 4 Results

Adsorption			Desorption				
ϕ_{in} (eV)	ϕ_{min} (eV)	$\sigma_{min} \times 10^{-14}$ (atoms/cm^2)	ϕ_{min} (eV)	T_{min} (°K)	ϕ_{max} (eV)	V_{screen} (V)	F_{tip} (MV/cm)
4.52	1.52	1.90	1.52	510	4.52	100	-0.94
4.88	1.35	2.10	1.35	470	4.67	0	0
5.07	1.06	2.10	1.20	540	4.74	100	-0.94
5.14	1.03	2.10	1.03	520	5.06	-200	1.87

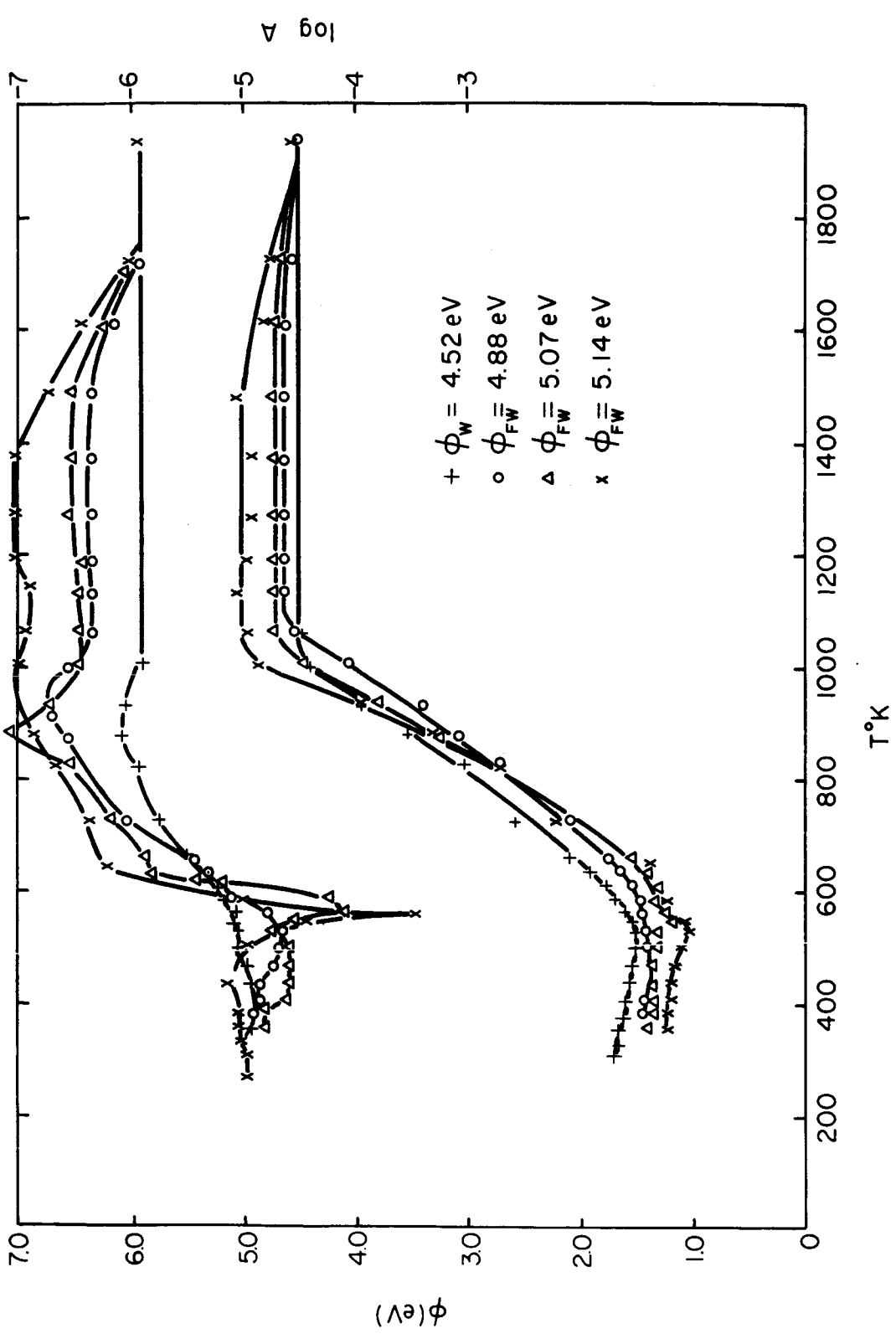

Figure 4. Plots show variation of ϕ (lower set of curves) and log A with 60 second heating at indicated temperatures for Cs on clean and fluorine coated tungsten. Bias voltages applied during each desorption sequence are given in Table II.

If the F remains on the surface throughout the adsorption-desorption sequence, ϕ_{max} should equal the initial work function ϕ_{in}. According to Figure 4, this appears to be true only for ϕ_{FW} = 5.14 eV where the screen was held at a negative potential during heating. The curve for the ϕ_{FW} = 5.07 eV layer, whose adsorption sequence was nearly the same as ϕ_{FW} = 5.14 eV, did not go through the same minimum work function on desorption, indicating some sort of irreversibility. The application of 100V to the screen during heating, as was the case for the clean W and ϕ_{FW} = 5.07 eV, returns Cs^+ to the emitter surface and causes Cs desorption to occur only in neutral form. On the other hand, the curve for the ϕ_{FW} = 5.14 eV in which -200V was applied during heating allows Cs^+ to be removed if the energetics are favorable.

Because of the different biases applied to the screen during the heating sequences, a proper trend in the desorption temperatures with ϕ_{FW} cannot be clearly established. Comparing the two curves in which 100V was applied to the screen so that only neutral Cs was permitted to desorb, we note that the ϕ_{FW} = 5.07 eV curve lies to the right of the clean W curve, thus indicating an enhanced binding of Cs to the fluorinated surface. Further measurements of Cs desorption rates as a function of ϕ_{FW} will be necessary to establish this point.

DISCUSSION

The Cs/F/W system exhibits most of the features of the analogous Cs/O/W system. Both systems exhibit a lower work function than the Cs/W system; they both diminish the surface diffusion rates of Cs on the respective surfaces, certain pattern similarities are noted between the two systems[4] and the stability of Cs with respect to thermal desorption appears to be increased with underlying O or F. There are however, some significant differences between these two systems which indicate the Cs/F/W system is less stable under certain conditions than the Cs/O/W system.

The ability to remove F^- by field desorption was pointed out earlier.[4] An examination of the energetics involved in field desorption of negative ions leads to the following expression for the activation energy E of desorption:

$$E = E_o + \phi - A_e - e^{3/2} F_a^{1/2} + aF_a + bF_a^2 \qquad (6)$$

where the symbols have the following meaning: E_o - zero field activation energy of desorption, A_e - electron affinity of F, e - electronic charge, a and b - constants. Accordingly, negative ion desorption becomes favorable at the low ϕ values obtainable by this system at high Cs coverages. The much larger value of A_e for F than for O is undoubtedly the main reason why the Cs/O/W system does not exhibit negative ion field desorption.

Another instability discovered in the Cs/F/W system was the ability of Cs to enhance the removal of F during thermal desorption. Table II shows that thermal desorption in the absence or presence of an applied negative field results in a net loss of F in all cases. As shown in Figure 4, the terminal desorption temperature for cesium removal occurs between 1000 and 1100°K, whereas thermal desorption of F takes place above 1400°K. However, upon application of a sufficiently large positive electric field, Cs is removed without concomitant F removal. This feature is shown more strikingly in Figure 5 where log A is plotted against ϕ for adsorption and desorption sequences on a clean W substrate and a F/W surface. Notice that adsorption and desorption points coincide for Cs on clean W indicating complete reversibility. With an underlying F/W layer such that $\phi \simeq 5.1$ eV, desorption in one case with a positive field and in the other case with a negative field applied results in a region of irreversibility at $\phi \simeq 2.0$ eV on both curves and at $\phi \gtrsim 3.5$ eV on the curve with the negative applied field. The cause of the slight irreversibility at $\phi \simeq 2.0$ eV is not obvious; however, the irreversibility occurring at $\phi \gtrsim 3.5$ eV for the negative field case (and which also occurs for the zero field case) is due to F removal. From Figure 4 we observed that $\phi \simeq 3.5$ eV corresponds to 900°K, well below the thermal desorption temperature of F alone.

The explanation of Cs induced F removal can be found by examining the possible desorption paths which are as follows:

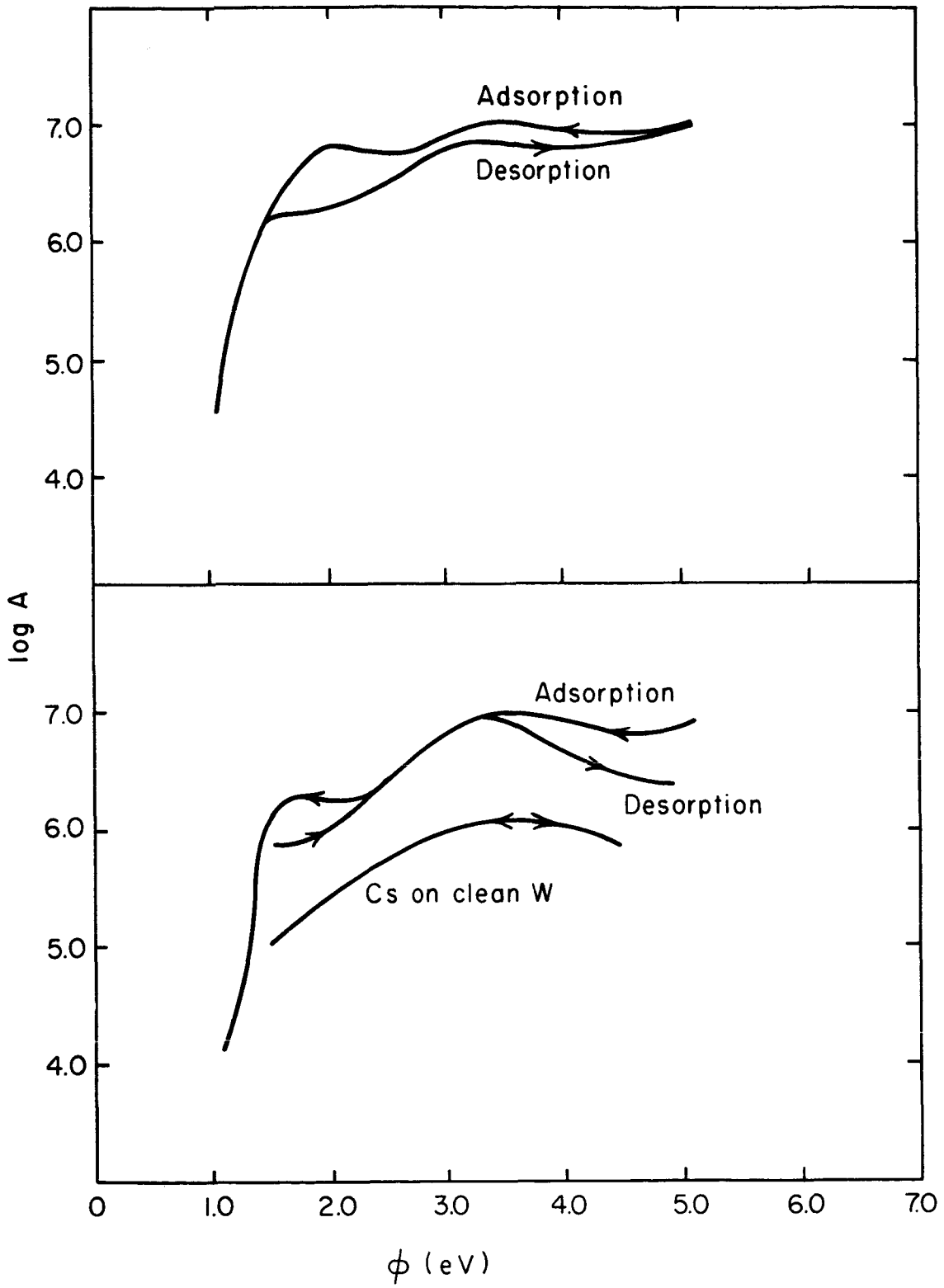

Figure 5. The upper set of curves show a plot of ϕ versus log A for a Cs adsorption desorption sequence, where $\phi_{FW} = 5.14$ eV and a negative voltage of 200 V was applied to the screen during tip heating. The lower set of curves is a similar plot where $\phi_{FW} = 5.07$ eV and a positive voltage of 100 volts was applied to the screen during tip heating. A 200 V positive bias voltage was applied to the screen for the clean W desorption sequence of Cs.

$$CsFW \xrightarrow{E_1} Cs + FW \quad (1)$$

$$CsFW \xrightarrow{E_2} CsF + W \quad (2)$$

$$CsFW \xrightarrow{E_3} Cs^+ + FW^- \quad (3)$$

$$Cs\,W \xrightarrow{E_4} Cs + W \quad (4)$$

$$FW \xrightarrow{E_5} F + W \quad (5)$$

On the basis that a F/W surface is thermally stable up to 1400°K when Cs is absent means reaction 5 requires the highest value of activation energy E_5 of the above series. Wolf[3] measured the desorption energy of process 5 and obtained $E_5 = 6.4$ eV at near zero F coverage. Process 4 occurs throughout the coverage range and E_4 increases as σ^- decreases; in all cases Cs is completely removed in the temperature range 1000 to 1100°K. Process 1, which represents neutral Cs desorption from a F/W site can also occur in ionic form according to process 3. The energetics of surface ionization readily yield the relation

$$E_3 = E_1 + I - \phi \quad (7)$$

where I is the ionization potential of Cs. Since $I-\phi = 0$ when $\phi = 3.87$ eV, the condition $E_3 < E_1$ must hold for the coverage range corresponding to $\phi > 3.87$ eV. In order for process 2 to compete with 3 in this coverage range, we must show that $E_2 \tilde{=} E_3 = E_1 + I - \phi$. Assuming that process 1 involves breaking of a Cs/F bond, the value of E_1 is the order of the dissociation energy 5.5 eV , yielding

$$E_3 \tilde{=} 9.4 - \phi \quad (8)$$

when $\phi > 3.4$ eV it follows that in order for process 2 to compete with 3, the condition $E_2 \lesssim 6.0$ eV must hold. In view of the fact that process 2 involves the breaking of a F/W bond, the maximum value of E_2 is the order of the measured desorption energy which, according to Wolf[3], is 6.4 eV. Since

the latter was measured for terminal desorption, the value of E_2 at larger F coverages is likely to be smaller. Hence, the condition $E_2 \gtrsim 6.0$ eV is readily met and the removal of F via process 2 is plausible.

It now remains to explain why positive applied fields allow removal of Cs without concomitant removal of F. At sufficiently high positive fields, process 3 is enhanced by positive field desorption; that is, Equation (6) can be rewritten

$$E_3 = E_1 + I - \phi - e^{3/2} F_a^{1/2} + aF_a + bF_a^2 \qquad (9)$$

Since the terms linear and quadratic in F_a are normally small compared to the $F^{1/2}$ term, they can be neglected; thus, at a field strength of 1.8×10^6 V/cm, E_3 can be reduced by as much as 0.5 eV. Apparently the reduction in E_3 is sufficient to cause process 3 to compete favorably with 2 so that F is no longer removed in significant amounts during thermal desorption. Also, since process 2 involves a bimolecular reaction between Cs and F, the reduction of Cs coverage through process 3 reduces the kinetic favorability of process 2. Although the above interpretations are qualitative, their explanation of the experimental observations give them credence. One may ask why Cs does not enhance removal of O in the analogous Cs/O/W system. This can be explained primarily by the fact that the Cs/F bond is roughly 2.0 eV stronger than the Cs/O bond. When reflected through the previous arguments with the further fact that F/W and O/W bond energies are nearly the same, we find that processes 1 and 3 are more favorable than 2 for the Cs/O/W system.

CONCLUSION

In many ways the Cs/F/W system is identical to the Cs/O/W system. For example, both underlying F and O chemisorbed layers on W enhance the work function lowering, the binding of Cs to the substrate and diminishes the mobility of Cs at a given temperature. In addition, both underlying electronegative adsorbates cause a redistribution in the field emission current from that observed for Cs on clean W. An important difference between these two

systems is the fact that at high coverages where the work function is at its minimum the high value of A_e for F allows the occurrence of field desorption of F^- upon the application of negative applied fields, even at $78^{\circ}K$. Another difference occurs at the low coverage region where thermal desorption of Cs also promotes the removal of the normally stable F. This observation is of some practical concern, since the ability of F to increase the work function of the collector surface in thermionic convertors may be reduced by the cesium induced removal F from the refractory metal collector surface at elevated temperatures.

CATHODE LIFE STUDIES

INTRODUCTION

Initiation of a cathode life study of zirconium and oxygen coadsorbed on tungsten field emission cathodes was begun last period. Such a study seemed advantageous in order to gain some insight into the life and stability of low work function Zr/O/W coated tungsten field emission cathodes. The main interests lay in the determination of mechanisms involved in cathode coating deterioration during operation and the possibility of increasing the stability and life of such a cathode by minimizing effects contributing to coating deterioration. A study such as this must be of limited scope due to limitations of budget and time and cannot be an investigation into life expectancy determinations; since such a study involves statistical analysis of relatively large numbers of cathodes operated under a variety of conditions which, at this time, is neither feasible nor necessary. It was therefore decided that a single tube operated under a variety of conditions was sufficient to give some indication of mechanisms involved in limiting the stability and life of this type of coated cathode.

There are two physical processes by which field emitted current from a clean surface may vary with time. One is geometric changes in the emitter surface caused by bombardment of high energy positive ions. The other process involves work function change due to adsorption of neutral gas molecules on the emitter surface. Since ionic bombardment roughens the surface, microscopic protrusions are usually formed which enhance the local electric field and, hence, current. Gas adsorption, on the other hand, nearly always increases the emitter work function, thereby decreasing the field emission current. In the case of an adsorbate coated emitter which lowers the work function, ionic bombardment may not only roughen the surface, but also sputter the low work function adsorbate thus leading to a current decrease with time.

In view of the fact that current instability occurs even in high vacuum field emission tubes and is generally proportional to the emitted current magnitude, it appears plausible that both ionic and neutral bombardment of the emitter is caused by the now well-known process of electron induced desorption of ions and neutrals from anode surfaces.[6-8] The specific purpose of this study is to examine the origin of these ions by attempting to suppress ionic bombardment of the emitter and to vary the collected electron energy below the threshhold for electron induced desorption.

EXPERIMENTAL TUBE

A schematic diagram of the tube used in this experiment is shown in Figure 6. By operating the tube in an axial magnetic field, the emitted electrons may be confined to a small diameter beam and collected in a Faraday cup at various voltages. By using a Faraday cup with a screen grid in front of it, all secondary electrons created at the Faraday cup may be suppressed from returning to high voltage electrodes where ions may be created. A resistively heatable zirconium source also served as a "β" ring and was placed such that direct interception with the electron beam was impossible. The anode consisted of a tungsten disc, which was phosphor-coated for pattern viewing purposes and had a 1/4 inch diameter aperature in the center. The beam could be focused through the 1/4 inch hole when immersed in the magnetic field and collected at low voltage in the Faraday cage.

The tube was operated in two basic modes. One mode was a simple diode in which all elements, except the tip assembly, were tied electrically to the anode voltage. In this mode of operation ions and neutrals formed at the anode could return to the negative emitter assembly. In the other mode of operation the "β" ring was employed as the anode, the phosphor-coated electrode and surpressor electrode were operated in the voltage range 20 - 50 V so as to maximize current collection at the Faraday cup and minimize current collection elsewhere. Also the collector voltage was varied continuously in order to examine the effect of collected electron energy on emitter stability.

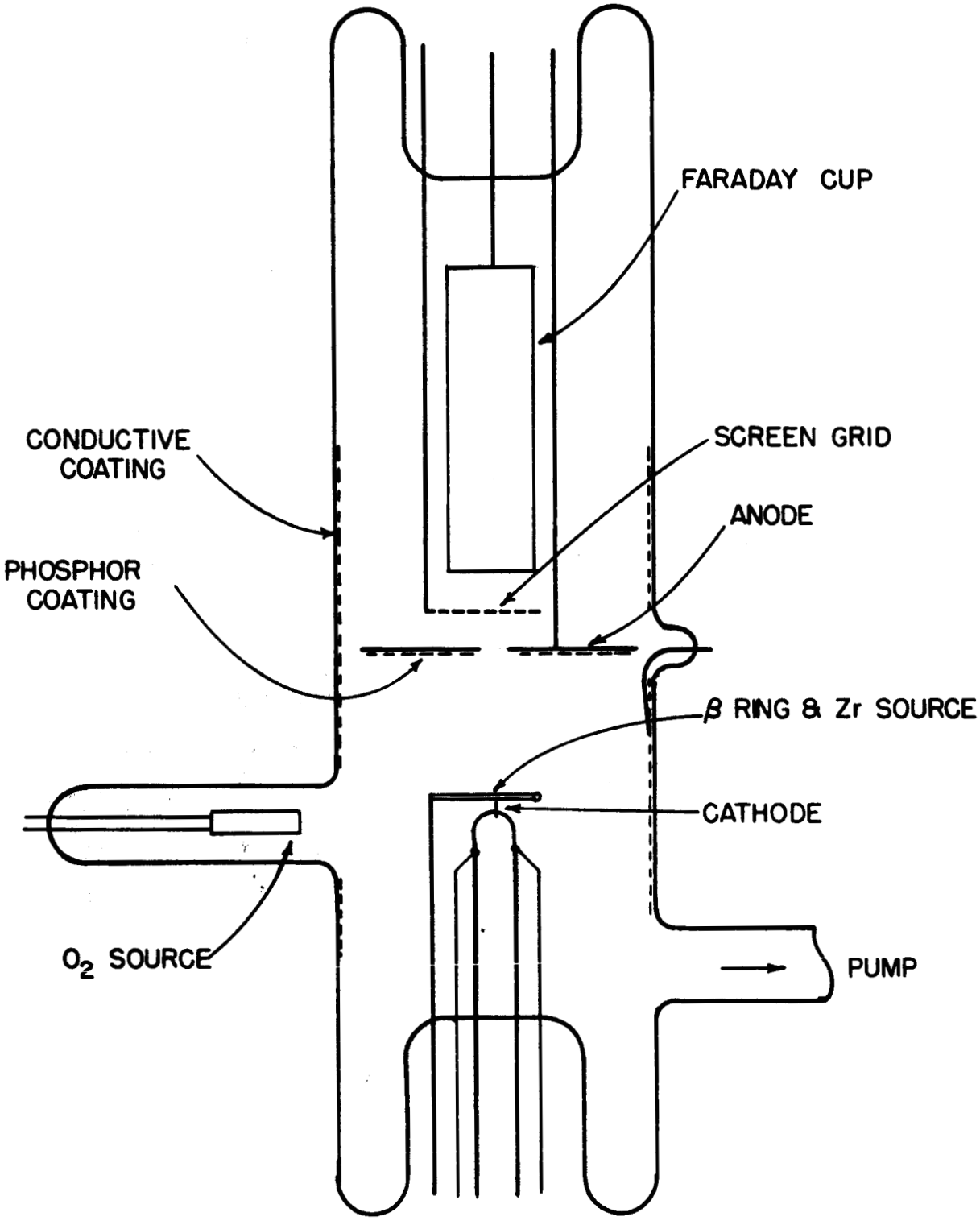

Figure 6 Diagram of tube designed to eliminate ion bombardment of the cathode.

The primary reason for operating the phosphor-coated electrode at low voltages in this mode of operation was due to the fact that beam transmission through the aperature was maximized. It should also be pointed out that in this operational mode a positive potential hump formed by the β ring served as a barrier for ions formed on other electrode elements to return to the emitter.

RESULTS

The emitter was coated with a low work function Zr/O coating by heating the poorly outgassed Zr source after which the tube was operated at ~1.5 μA for 10 to 15 minute periods with various collection voltages on the Faraday cup. The current was monitored continuously for each voltage so that a plot could be made of current vs time. From this graph an average value of dI/dt could be obtained for each voltage on the Faraday cup in order to obtain a rate of current change. It was then possible to plot dI/dt vs collector voltage in order to measure the stability of the emitted current as a function of voltage at which the electrons were collected. The tube was also operated as a simple diode at the same current as previously mentioned without any attempt to suppress electron ion tip bombardment. A value of $(dI/dt)_o$ could be found for this mode of operation and compared with each dI/dt data point found previously to obtain a percentage of improvement of stability (i.e., $1 - (dI/dt)/(dI/dt)_o$) with respect to diode operation as shown in Figure 7. The points in excess of 100% represent a reversal in sign of dI/dt. Also shown in Figure 6 is the fraction of total current I_t being collected at the β ring I_β. The current I_β originates from reflected primaries or secondaries from the phosphor coated electrode.

CONCLUSIONS

The data obtained in this experiment yields some interesting evidence of the effects of the stability of zirconium-oxygen surface coatings on tungsten field emitters. First, it must be pointed out that the relationship between operating conditions of the ion suppression mode and the simple diode mode

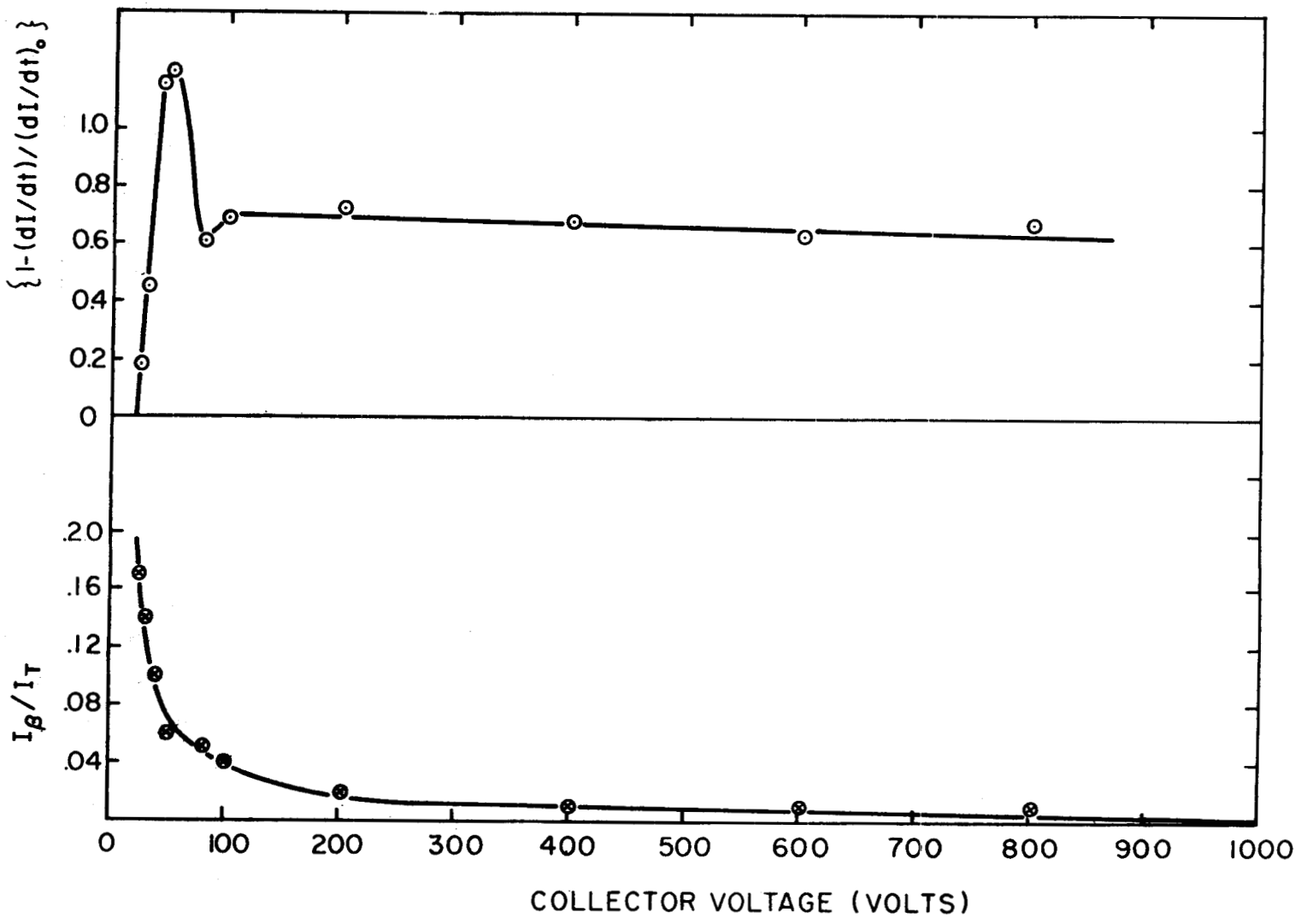

Figure 7. The upper curve shows the percent increase in time stability of the field emission current over straight diode operation when the current is collected at the various indicated voltages. The lower curve shows the ratio of current collected at the β-ring to total current as the collector voltage is increased. The value of I_t was 1.5 μA throughout the voltage range.

are quite different. When operated in the ion suppression mode nearly all electrons are collected in a Faraday cup on clean metal surfaces, whereas operation in the diode mode at V =960V did not limit electron collection to any one surface. Metal, phosphor coated metal and tin oxide coated glass were all bombarded by high-voltage electrons in the diode mode, so it is not surprising that a 60 to 70% improvement in current stability is observed between the two modes of operation, due to the difference in cleanliness of the surfaces bombarded. Figure 7 shows that very little improvement in cathode deterioration rate was observed between collection voltages of 800 and 100 volts. This is probably a result of the fact that ion bombardment has been practically eliminated, and the effect of neutral capture by the tip results in a constant rate of coating deterioration in this voltage range. It is also shown in Figure 7 that a small fraction of the total current is not collected in the Faraday cup and is either reflected or creates secondaries which return to the "β" ring where ions and neutrals can be created by electron bombardment, neither of which can be prevented from striking the tip. Between 100 and 50 volts the coating deterioration rate improves rapidly and the rate of change of dI/dt becomes positive. This effect appears to be the result of approaching the threshhold for electron induced desorption of gas atoms from the bombarded surface, resulting in a rapid decrease in the neutrals returning to the tip. Ion bombardment of the tip is not changed however, since ions originating at the β ring can continue to bombard the emitter. Apparently there is a balancing of effects---on one hand, ion bombardment, which causes an increase in current due to surface roughening, and on the other, neutral adsorption, which causes a decrease in current due to an increase in work function. The rapid change of direction of the cathode deterioration rate between 0 and 50 volts seems to be the result of the effect of space charge enlarging the electron beam, and thereby increasing I_β / I_t such that the deterioration rate approaches that of diode operation. The close proximity of the β ring to the emitter probably enhances the deterioration rate.

It seems reasonable to assume that two effects involved in the current

instability of Zr/O/W coated field emitters are neutral and ion bombardment of the tip during operation. Neutral adsorption apparently causes a negative dI/dt whereas ionic bombardment causes a positive dI/dt. More stable operation of this type of cathode coating should result by collecting electrons on low voltage, clean surfaces in order to reduce the probability of electron desorption of adsorbed gases. The presence of a positive potential hump in front of the cathode also appears to aid in increasing the stability of the Zr/O/W surface.

REFERENCES

1. L. W. Swanson, et al, Final Report for NASA Contract NASw-458 (Field Emission Corporation, 1963).

2. L. W. Swanson, et al, Final Report for NASA Contract NAS3-2596 (Field Emission Corporation, 1964).

3. E. D. Wolf, 25th Ann. Conf. on Physical Electrons, M. I. T. (1965) and private communication (1966).

4. L. W. Swanson, et al, Final Report for NASA Contract NASw-1082 (Field Emission Corporation, 1966).

5. J. B. Taylor and I. Langmiur, Phys. Rev. 44, 423 (1933).

6. D. Zimmerman and R. Gomer, Rev. Sci. Instr. 36, 1046 (1965).

7. D. Menzel and R. Gomer, J. Chem. Phys. 41, 3329 (1964).

8. D. Menzel and R. Gomer, J. Chem. Phys. 41, 3311 (1964).

9. P. Redhead, Vacuum 13, 253 (1963).

QUARTERLY DISTRIBUTION LIST

Contract NASw 1516

NASA Headquarters Washington, D. C. 20546 Attn: Dr. R. R. Nash - Code RRM	4
G. Pfannebecker - Code RNT	1
T. Tsacoumis - Code REG	1
Scientific and Technical Information Facility Attn: NASA Representative Post Office Box 5700 Bethesda, Maryland 20014	2
NASA Lewis Research Center Cleveland, Ohio 44135 Attn: Dr. R. Breitweiser, Section 2131	1
Dr. R. A. Lad, Section 2330	1
J. Ferrante, Section 9711	1
D. L. Lockwood, Section 9711	1
Dr. J. F. Morris, Section 1951	1
Dr. H. Schwartz, Section 9213	1
Dr. L. Tower, Section 2132	1
NASA Marshall Space Flight Center Huntsville, Alabama Attn: Dr. I. Dalins, Code R-RP-N	1
NASA Electronic Research Center Cambridge, Massachusetts Attn: Dr. M.S. Macrakis, Code CT	1
U.S. Naval Ordnance Test Station Physics Division, Michaelson Laboratory China Lake, California 93556 Attn: Dr. E. Bower, Head Crystal Physics Branch	1
National Bureau of Standards Atomic Physics Division Washington, D. C. 20546 Attn: Dr. R. D. Young Electron Physics Section	1

Professor Robert Gomer
Institute for the Study of Metals
University of Chicago
Chicago, Illinois 60637 1

Professor W. L. Boeck
Department of Physics
Niagara University
Niagara University, New York 14109 1